Dipole radiation in a one-dimensional photonic crystal: TE polarization

I. Alvarado-Rodriguez*
Instituto Nacional de Astrofísica, Óptica y Electrónica, Apartado Postal 51, Puebla, Puebla 72000, Mexico and Centro de Investigaciones en Ingenieria y Ciencias Aplicadas, Universidad Autónoma del Estado de Morelos, Avenida Universidad 1001 Col. Chamilpa, Cuernavaca 62210, Mexico

P. Halevi† and Adán S. Sánchez
Instituto Nacional de Astrofísica, Óptica y Electrónica, Apartado Postal 51, Puebla, Puebla 72000, Mexico
(Received 30 August 2000; published 24 April 2001)

We study the power emitted by an oscillating dipole in a superlattice (SL) modeled by means of a periodic distribution of Dirac δ functions (*Dirac comb* SL). The radiation is permitted to propagate in all directions in space; however, it is restricted to the transverse electric (TE) polarization mode. The calculation is based on a classical theory of radiation in nonuniform dielectric media by Dowling and Bowden [Phys. Rev. A **46**, 612 (1992)]. The emitted power is derived in terms of a single integral, with no approximations. A SL has no omnidirectional photonic band gaps, and therefore the power is always finite. The power spectrum exhibits slope discontinuities, which occur at the band edges for on-axis propagation. It also depends strongly on the dipole's position in the SL and on the *grating strength* that characterizes the Dirac comb model. The power peaks for low frequencies, and there can be large enhancement of emission as compared to free space. The closer the dipole is to a *barrier* (Dirac δ) and the greater the grating strength, the stronger the enhancement is. These conclusions are expected to be relevant for a real SL.

DOI: 10.1103/PhysRevE.63.056613 PACS number(s): 42.70.Qs, 42.50.Gy

I. INTRODUCTION

In a pioneering paper, Purcell pointed out that the spontaneous emission (SE) by an atom is altered if the radiated field is constrained to satisfy a set of boundary conditions [1]. In other words, the lifetime of an excited atomic state changes if the atom is located in a material environment, rather than radiating in free space. Consider, for example, an atom enclosed in a loss-free cavity. It is well known that such a cavity supports a series of eigenmodes whose characteristic frequencies $\omega_1, \omega_2, \ldots$ depend only on the geometry of the cavity. If none of these frequencies matches the (free-space) emission spectrum of the atom, then it will find no eigenmode to decay into. The atom will then be unable to radiate. More generally, if the material surroundings are such that the modal density (or density of optical states) vanishes, then the spontaneous emission is prohibited. If the density of states (DOS) is merely reduced with respect to the free space value, then the spontaneous emission is inhibited. On the other hand, an enhancement of the emission is also feasible. This is the essence of the Purcell effect, and it has stimulated the development of cavity quantum electrodynamics (QED) dedicated to radiative properties of atoms between two mirrors or within other cavities. We quote two reviews of this field [2] and a few recent papers [3].

Photonic crystals (PCs) [4] are novel, composite materials that offer an attractive opportunity for studying SE by atoms, fluorescence by dyes, radiative recombination of electrons and holes, etc., in a very low DOS environment. A PC is a periodic array of (usually) two dielectric materials. In the case of a three-dimensional (3D) PC, appropriate geometrical characteristics and sufficiently large dielectric contrast between the two constituent materials may result in an omnidirectional photonic band gap (PBG). This is to say that, within the PBG, light is prohibited to propagate in whatever direction. Strictly speaking, this would require perfect periodicity (including an infinite PC) and lossless materials. Under such ideal conditions, as proposed by Yablonovitch, SE due to electron-hole recombination in a semiconductor—incorporated within the PC—could be prohibited provided that the recombination frequency (which is just the semiconductor's energy band gap, divided by Planck's constant) falls within the PBG [5]. This could greatly improve the performance of semiconductor lasers and other devices [5]. It is worth noting that the spontaneous emission rate due to electron-hole recombination in a GaAs film was found to increase or decrease markedly, depending on whether the substrate dielectric had a higher or lower refractive index than that of GaAs [6].

John and Wang studied SE by an atom whose transition frequency lies near a PBG [7]. Their QED theory predicts bound states of photons to hydrogenic atoms, namely, ''dressed atoms.'' In the vicinity of a photonic band edge, the excited atomic state undergoes an anomalous Lamb shift (due to the electron's interaction with the radiation field) and splits into a doublet. One member of this doublet gives rise to the aforementioned ''dressed atom,'' with the electromagnetic energy decaying exponentially away from the atom. The other member leads to fluorescence which, according to Kofman *et al.*, is characterized by the occurrence of beats, corresponding to a non-Lorentzian emission spectrum [8]. Several other studies explore the decay of a two-level atom in the presence of a PBG [9]. The radiative coupling of two

*Present address: Dept. of Electrical Engineering, University of California at Los Angeles, Los Angeles, CA 90024-7594.
†Email address: halevi@inaoep.mx

atoms or dipoles has been investigated by Kurizki [10], Dowling and Bowden [11], and Wang [12]. Further, John and Quang found that the collective SE by N two-level atoms inside a PC leads to the localization of superradiance near a PBG [13]. It was also shown by John and collaborators that the SE by a three-level atom, with one resonant frequency near a PBG edge, can be coherently controlled; this may be relevant for an optical memory device on the atomic scale [14]. Huang *et al.* investigated dressed states for a multilevel atom and localized field in a PC [15].

The aforementioned theoretical work [7–15] considers, by and large, strong coupling between the atom inside the PC and the electromagnetic field. As a result, so-called *Rabi oscillations* take place: for a two-level atom in a cavity, the probability of either state being occupied depends harmonically on time (the period of the oscillations is the *Rabi frequency*) [2,16]. What happens (in the idealized absorptionless situation) is that the excitation energy is exchanged periodically between the atom and the field. Such a state of affairs requires complicated QED theories, complete with creation and destruction operators. On the other hand, the experiments performed to date on PCs (see below) seem to involve only weak interaction between the emitting particles and the field. Then the so-called Weisskopf-Wigner approximation [17] is applicable, which results in great simplification, namely, the decay process becomes exponential in time. This point was emphasized by Li *et al.* [18], who very recently computed the ''local'' DOS (that incorporates the atom-field interaction) for a two-level atom embedded in a 3D PC. On the basis of realistic band-structure calculations, the authors concluded that the local DOS varies slowly near the band-gap edges—in contrast to the previous isotropic model [7]. This behavior seems to justify the Weisskopf-Wigner approximation for 3D PCs. Glauber and Lewenstein used this approximation in order to calculate the rate of spontaneous emission γ_s of an atom embedded in a nonuniform dielectric medium, characterized by an arbitrary, position-dependent dielectric constant $\epsilon(\mathbf{r})$ [19]. It turns out that the emitted power is independent of Planck's constant; hence it actually corresponds to semiclassical radiation theory. Then one can expect that a classical theory of radiation by a point dipole, with its dipole moment $\boldsymbol{\mu}$ replaced by the atomic dipole transition matrix element $\langle m|e\mathbf{r}|n\rangle$ will lead to the very same results. Such a theory, for arbitrary $\epsilon(\mathbf{r})$, was developed by Dowling and Bowden (DB) [20] and, indeed, the replacement $\boldsymbol{\mu}\rightarrow\langle m|e\mathbf{r}|n\rangle$ in Eq. (26) of Ref. [20] leads to the expression for $\hbar\omega_0\gamma_s$ derived by Glauber and Lewenstein [see Eq. (6.11a) of Ref. [19]] within a numerical factor.

DB applied their theory to the calculation of the power emitted by a point dipole located between a pair of perfect mirrors and also to a dipole embedded in a superlattice (SL) that was modeled by means of Dirac-delta functions (Dirac comb model). In both examples the radiation was assumed to propagate in the axial direction, corresponding to normal incidence [20]. The calculation for dipole radiation within the mirrors was generalized by Alvarado-Rodriguez *et al.* to allow for arbitrary direction of propagation and polarization [21]. Further, Tocci *et al.* [22], Fogel *et al.* [23], and Dowling [24] applied transfer matrix methods to the DB result in order to calculate the power emission by a dipole in a finite SL. Tocci *et al.* also compared their calculations to spontaneous emission spectra of a GaAs thin film at the middle of a $AlAs/Al_xGa_{1-x}As$ SL. They obtained reasonable agreement and enhancement by a factor 3.5 near the photonic band edge [22]. We also mention early work by Bykov [25] and calculations by Russell, *et al.* [26] that shows how SE can be controlled by placing a dipole inside a layer of low-index material, built into a dielectric SL (both TE and TM modes are considered). Babiker and collaborators considered a SL made up from dispersive layers, modeled so as to allow for the presence of phonon polaritons [27]. They found that the dipole relaxes by exciting TM-polarized polaritons localized at the interfaces between the layers.

Turning to PCs of 2D periodicity, Suzuki *et al.* embedded a radiowave dipole oscillator in a periodic array of dielectric rods [28]. They obtained quantitative agreement between the measured emitted power and a calculation based on the DB theory. Recently, SE from hexagonal microcavities surrounded by triangular arrays of holes (in a membrane structure) was observed by Lee *et al.* [29] and by Boroditsky *et al.* [30] at a wavelength ~ 1.5 μm. In both, rather similar experiments, the active regions—$In_xGa_{1-x}As$ quantum wells (that constituted the cavity)—were pumped by lasers and photoluminescence spectra were taken for light emitted perpendicular to the membranes. Twofold [29] and sixfold [30] enhancements of the light extraction efficiency were demonstrated in comparison to the unpatterned membrane. Baba *et al.* also observed strong enhancement for GaInAsP microcolumn arrays [31].

As for 3D structures, Suzuki and Yu modified the DB method in order to calculate the emitted power of a dipole inside a PC with face-centered cubic structure [32]. The results show prohibition of emission in the PBG and also strong enhancement near the band edges. On the experimental side, there are many papers on self-organizing microspheres, made of polystyrene or silica (artificial opal), that crystalize in diverse space lattices [33]. These dielectric materials have small dielectric constants, so there is no omnidirectional PBG, but only a pseudogap. Therefore, when doped with a fluorescent dye or a semiconductor, these PCs exhibit merely moderate inhibition of SE. What makes them attractive is that this occurs in the visible regime.

In this and the next paper [34] we calculate the power emission, by an oscillating point dipole, in a perfect SL. The SL is modeled by means of a periodic distribution of Dirac delta functions—the Dirac comb model. As mentioned before, this elegant model was first introduced in the DB paper [20]. There, however, the light was restricted to propagate along the SL axis. In practice, a dipole or an atom will radiate in all spatial directions, and here we generalize the DB calculation so as to allow for this feature. We employ the DB theory, which expresses the emitted power in terms of the normal modes of the system. For a SL, these are the TE and TM modes; the corresponding eigenvalue problems for the Dirac comb model were solved by Alvarado-Rodriguez *et al.* [35] and Zurita and Halevi [36]. In these two papers we derived the band structures, fields, equifrequency surfaces,

and the DOSs for the two polarizations. These results will be used in the calculation of the power emitted into the TE modes (this paper) and into the TM modes (next paper) [34]. We also calculate the power emitted by a gas of dipoles within the superlattice. In general, the calculation of power emission by a dipole or an atom embedded in a PC is a difficult problem. The Dirac comb model, while unrealistic from the quantitative point of view, has the advantages of simplicity and transparency. In fact, exact final results are derived in terms of a single integration.

In Sec. II we briefly review the DB theory for radiation in an arbitrarily inhomogeneous dielectric medium. The results of Ref. [35] for the TE modes of the Dirac comb SL are recapitulated in Sec. III. The electric field is normalized in Sec. IV, and in Sec. V we calculate the emitted power. Special cases, including the power radiated by a gas of dipoles, are considered in Sec. VI. Our numerical results are presented and analyzed in Sec. VII.

II. POWER EMISSION IN AN INHOMOGENEOUS MEDIUM

In this section we recapitulate the modal radiation theory of Glauber and Lewenstein [19], according to its classical rendition by Dowling and Bowden [20]. We start with the wave equation for the vector potential $\mathbf{A}(\mathbf{r},t)$. In the absence of sources, it is

$$\boldsymbol{\nabla}\times\boldsymbol{\nabla}\times\mathbf{A}+\frac{\epsilon(\mathbf{r})}{c^2}\frac{\partial^2}{\partial t^2}\mathbf{A}=\mathbf{0}. \tag{1}$$

Here the dielectric constant $\epsilon(\mathbf{r})$ is a function of the position vector $\mathbf{r}$ due to the inhomogeneity. The vector potential fulfills the Coulomb or transverse gauge

$$\boldsymbol{\nabla}\cdot[\epsilon(\mathbf{r})\mathbf{A}]=0 \tag{2}$$

rather than $\boldsymbol{\nabla}\cdot\mathbf{A}=0$ as in an homogeneous medium. For a given material geometry, we can describe the field therein as a linear superposition of normal modes or eigenmodes. Each mode may be labeled according to its wave vector $\mathbf{k}$ and polarization index p. So, the total monochromatic field present in the medium is given by

$$\mathbf{A}(\mathbf{r},t)=\sum_p\sum_{\mathbf{k}}\mathbf{a}_{\mathbf{k}p}(\mathbf{r})\exp(-i\omega_{\mathbf{k}p}t)\,\delta(\omega_{\mathbf{k}p}-\omega_0). \tag{3}$$

Here $\omega_{\mathbf{k}p}$ and $\mathbf{a}_{\mathbf{k}p}(\mathbf{r})$ are the eigenfrequency and eigenvector of the $\mathbf{k},p$ mode. The Dirac δ function ensures that the fields oscillate only at source frequencies ω_0 that the inhomogeneous medium can admit, namely the eigenfrequencies $\omega_{\mathbf{k}p}$. These normal modes are monochromatic solutions of the Helmholtz equation, obtained by substituting Eq. (3) in Eq. (1)

$$\boldsymbol{\nabla}\times\boldsymbol{\nabla}\times\mathbf{a}_{\mathbf{k}p}(\mathbf{r})-\frac{\omega_{\mathbf{k}p}^2}{c^2}\epsilon(\mathbf{r})\mathbf{a}_{\mathbf{k}p}(\mathbf{r})=\mathbf{0}. \tag{4}$$

The eigenvectors $\mathbf{a}_{\mathbf{k}p}(\mathbf{r})$ also have to fulfill the normalization and closure conditions given by the following equations:

$$\int d^3r\,\epsilon(\mathbf{r})\mathbf{a}^{\star}_{\mathbf{k}'p'}(\mathbf{r})\cdot\mathbf{a}_{\mathbf{k}p}(\mathbf{r})=\delta(\mathbf{k}-\mathbf{k}')\,\delta_{pp'}, \tag{5}$$

$$\sum_{p=1}^{2}\int d^3k\,\mathbf{a}^{\star}_{\mathbf{k}p}(\mathbf{r}')\mathbf{a}_{\mathbf{k}p}(\mathbf{r})=\overleftrightarrow{\delta}(\mathbf{r}-\mathbf{r}'). \tag{6}$$

Note that both sides of the last equation are dyadics. Equations (5) and (6) ensure that the $\mathbf{a}_{\mathbf{k}p}(\mathbf{r})$ are a complete set of orthonormal functions.

Next, the inhomogeneous wave equation for a source localized in space must be solved,

$$\boldsymbol{\nabla}\times\boldsymbol{\nabla}\times\mathbf{A}+\frac{\epsilon(\mathbf{r})}{c^2}\frac{\partial^2}{\partial t^2}\mathbf{A}=\frac{4\pi}{c^2}\mathbf{J}. \tag{7}$$

Here $\mathbf{J}(\mathbf{r},t)$ is a current density corresponding to a pointlike dipole, namely,

$$\mathbf{J}(\mathbf{r},t)=\omega_0\boldsymbol{\mu}\cos(\omega_0 t)\,\delta(\mathbf{r}-\mathbf{r}_0)\Theta(t). \tag{8}$$

The dipole has a moment $\boldsymbol{\mu}$, is located at the point $\mathbf{r}_0$, is oscillating with frequency ω_0, and is turned on at the time $t=0$, as evident from the step function $\Theta(t)$. Equation (7) can be solved in terms of the normal modes as given in Eq. (3), and then one can calculate the work done by the dipole current against the ambient electric field to find the radiated power. Following the procedure in Ref. [20], the power radiated by the point dipole in the steady state is

$$P=\pi^2\omega_0^2\mu^2\sum_{p=1}^{2}\int d^3k|\mathbf{a}_{kp}(\mathbf{r}_0)\cdot\hat{\boldsymbol{\mu}}|^2\,\delta(\omega_{\mathbf{k}p}-\omega_0), \tag{9}$$

where $\hat{\boldsymbol{\mu}}$ is a unit vector parallel to μ. Equation (9) implies that the power emitted by the point radiator depends on the normal modes being excited. The Dirac δ function selects the modes that have the frequency of the radiator and therefore contribute to the radiated power. The total power can be decomposed into independent contributions from each polarization mode. Hence one can study separately the contributions $p=\mathrm{TE}$ and $p=\mathrm{TM}$. Because this paper is restricted to the former case, we can drop the mode index p.

III. TE NORMAL MODES

We consider a dielectric SL modeled by means of the Dirac comb [20], Fig. 1:

$$\epsilon(x)=\epsilon_0+gd\sum_{n=-\infty}^{\infty}\delta(x-nd). \tag{10}$$

Here d is the period of the lattice, g is the ''grating strength,'' and ϵ_0 is the dielectric constant between the ''barriers'' located at $x=nd$. Formerly we derived the following dispersion relation for the TE propagation modes [35]:

$$\cos k_B d=\cos Kd-\alpha(\omega,K)\sin Kd, \tag{11}$$

$$K=\left(\frac{\omega^2}{c^2}\epsilon_0-k_{\parallel}^2\right)^{1/2}, \tag{12}$$

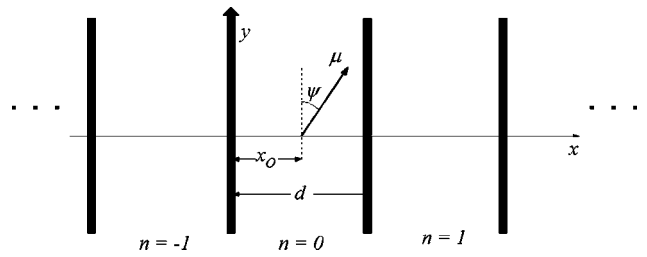

FIG. 1. Oscillating dipole in a Dirac comb superlattice; the dielectric constant is infinite on the periodically situated planes $x=\cdots -d,0,d,\ldots$, and it is equal to ϵ_0 between these planes. The dipole moment μ lies in the xy plane and forms an angle ψ with the y axis; the point dipole is distanced x_0 from the origin.

$$\alpha(\omega,K)=\frac{gd\omega^2}{2c^2K}. \tag{13}$$

Equation (11) is an implicit equation for the frequency, $\omega_{\mathbf{k}}=\omega(k_B,k_\parallel)$, as a function of the Bloch vector k_B and the wave vector component $k_\parallel$ in the plane parallel to the barriers. The corresponding band structure reasonably resembles that obtained from the realistic model of the SL, see Fig. 2 of Ref. [35].

The electric field of the TE mode is perpendicular to the SL axis and was found to be

$$\mathbf{E}_{\mathbf{k}}^{(n)}(x)=e^{ink_Bd}[Ae^{iK(x-nd)}+Be^{-iK(x-nd)}]e^{i(k_yy+k_zz)}\hat{\mathbf{e}}_{\mathbf{k}}, \tag{14}$$

$$\hat{\mathbf{e}}_{\mathbf{k}}=-\hat{\mathbf{y}}\cos\phi+\hat{\mathbf{z}}\sin\phi. \tag{15}$$

Here $\hat{\mathbf{e}}_{\mathbf{k}}$ is the polarization vector, that is, it is a unit vector in the yz plane that is perpendicular to $\mathbf{k}_\parallel$, which forms an angle ϕ with the z axis. This equation gives the field at any point x between the nth and the $(n+1)$th barriers, namely,

$$nd<x<(n+1)d. \tag{16}$$

Finally, the amplitudes A and B are related as

$$\frac{B}{A}=-\frac{1-e^{i(K-k_B)d}}{1-e^{-i(K+k_B)d}}. \tag{17}$$

Note that K, defined by Eq. (12), may have imaginary, as well as, real values. If $K=i|K|$, as occurs for sufficiently large values of $k_\parallel$, then in Eq. (11) the trigonometric functions of Kd must be replaced by the corresponding hyperbolic functions of $|K|d$. The parameter $\alpha(\omega,K)$, Eq. (13), becomes $\alpha(\omega,|K|)$. In this regime of imaginary K, the electric field, Eq. (14), has evanescent behavior $\exp(\pm|K|x)$.

IV. MODE NORMALIZATION

To proceed with the power calculation the eigenvectors of Eq. (14) have to be normalized. Now, the formula for the power, Eq. (9), requires the vector potential; we relate it to the electric field using the gauge Eq. (2) which, in the absence of charges, implies that the scalar potential vanishes. Then

$$\mathbf{E}_{\mathbf{k}}(\mathbf{r})=i\frac{\omega_{\mathbf{k}}}{c}\mathbf{a}_{\mathbf{k}}(\mathbf{r}), \tag{18}$$

and using Eq. (14) we have that

$$\mathbf{a}_{\mathbf{k}}^{(n)}(\mathbf{r})=-i\frac{c}{\omega_{\mathbf{k}}}e^{ink_Bd}[Ae^{iK(x-nd)}+Be^{-iK(x-nd)}]e^{i(k_yy+k_zz)}\hat{\mathbf{e}}_{\mathbf{k}}. \tag{19}$$

Written out explicitly, the normalization condition Eq. (5) becomes

$$\cdots+\int_{-\infty}^{\infty}dydz\int_{-d}^{0}dx\,\epsilon_0\mathbf{a}_{\mathbf{k}'}^{(-1)*}\cdot\mathbf{a}_{\mathbf{k}}^{(-1)}+\int_{-\infty}^{\infty}dydz\int_{0}^{d}dx\,\epsilon_0\mathbf{a}_{\mathbf{k}'}^{(0)*}\cdot\mathbf{a}_{\mathbf{k}}^{(0)}+\int_{-\infty}^{\infty}dydz\int_{d}^{2d}dx\,\epsilon_0\mathbf{a}_{\mathbf{k}'}^{(1)*}\cdot\mathbf{a}_{\mathbf{k}}^{(1)}+\cdots=\delta(\mathbf{k}-\mathbf{k}'). \tag{20}$$

By using the phase factor $\exp(ink_Bd)$ in Eq. (19), this can be reduced to an expression that involves only the cell $n=0$, and we get

$$\epsilon_0\sum_{n=-\infty}^{\infty}e^{in(k_B'-k_B)d}\int_{-\infty}^{\infty}dydz\int_{0}^{d}dx\,\mathbf{a}_{\mathbf{k}'}^{(0)*}\cdot\mathbf{a}_{\mathbf{k}}^{(0)}=\delta(\mathbf{k}-\mathbf{k}'). \tag{21}$$

Next we substitute Eq. (19) in Eq. (21). The integrals over y and z lead to $2\pi\delta(k_y-k_y')$ and $2\pi\delta(k_z-k_z')$, respectively. Because $\Sigma_{n=-\infty}^{\infty}e^{in(k_B-k_B')d}=2\pi\delta(k_B-k_B')/d$ we obtain, for real K, that

$$\frac{(2\pi)^3}{d}\frac{c^2}{\omega_{\mathbf{k}}^2}\epsilon_0\int_0^d dx[|A|^2+|B|^2+2\,\mathrm{Re}(A^*Be^{-2iKx})]\times\delta(k_B-k_B')\delta(k_y-k_y')\delta(k_z-k_z')=\delta(\mathbf{k}-\mathbf{k}'). \tag{22}$$

Canceling out the Dirac δ functions and integrating we find that

$$|A|^2+|B|^2+2\,\mathrm{Re}\left[A^*B\frac{e^{-2iKd}-1}{-2iKd}\right]=\frac{\omega_{\mathbf{k}}^2}{(2\pi)^3c^2\epsilon_0}. \tag{23}$$

Then substituting Eqs. (11) and (17) into Eq. (23) the result is

$$|A|^2=\frac{\omega_{\mathbf{k}}^2}{16\pi^3c^2\epsilon_0}\frac{\sin Kd+\alpha\cos Kd+\sin k_Bd}{\sin Kd+\alpha\cos Kd-\alpha\dfrac{\sin Kd}{Kd}},\quad K\ \text{real}. \tag{24}$$

If, on the other hand, K is imaginary, then we must replace $\exp(\pm iKx)$ in Eq. (19) by $\exp(\mp|K|x)$. Retracing the steps leading to Eq. (22), the expression in the square bracket is replaced by

$$[|A|^2 e^{-2|K|x} + |B|^2 e^{2|K|x} + 2\,\mathrm{Re}(A^* B)].$$

After integration over x, we obtain

$$|A|^2 = \frac{\omega_{\mathbf{k}}^2}{16\pi^3 c^2 \epsilon_0} \frac{\alpha(\sinh|K|d + \cosh|K|d)}{\sinh|K|d - \alpha\cosh|K|d + \alpha\dfrac{\sinh|K|d}{|K|d}},$$

$$K \text{ imaginary.} \tag{25}$$

Here α is given by Eq. (13), with the replacement $K \to |K|$. We note that Eq. (25) cannot be obtained from Eq. (24) by the substitution $K = i|K|$.

V. EMITTED POWER

To calculate the power radiated into the TE polarization mode, we use Eq. (9). Now we take the medium between the barriers to the vacuum ($\epsilon_0 = 1$). This is in order to avoid the complications due to the *local field* acting on a dipole within a dielectric medium. Without loss of generality, we assume that the dipole moment is parallel to the xy plane, namely, $\hat{\boldsymbol{\mu}} = \hat{\mathbf{x}}\sin\psi + \hat{\mathbf{y}}\cos\psi$, and that it is located within the cell labeled $n = 0$ at a distance x_0 from the barrier (see Fig. 1). With the help of the Eqs. (19) and (15) we find that the dipole-field interaction is given by

$$|\mathbf{a}_{\mathbf{k}}(\mathbf{r}_0)\cdot\hat{\boldsymbol{\mu}}|^2 = \frac{c^2}{\omega_{\mathbf{k}}^2}[|A|^2 + |B|^2 + 2\,\mathrm{Re}(A^* B e^{-2iKx_0})]\cos^2\psi\cos^2\phi. \tag{26}$$

In cylindrical coordinates $\mathbf{k} = (k_\parallel, \phi, k_B)$ and $d^3k = (k_\parallel d\phi)dk_\parallel dk_B$. Then Eq. (9) becomes

$$P = \pi^2 c^2 \mu^2 \cos^2\psi \int dk_\parallel k_\parallel \int d\omega \frac{dk_B}{d\omega} \int d\phi \cos^2\phi [|A|^2 + |B|^2 + 2\,\mathrm{Re}(A^* B e^{-2iKx_0})]\delta(\omega_{\mathbf{k}} - \omega_0). \tag{27}$$

For the Dirac δ function in the integrand we use the property

$$\delta(f(x)) = \sum_{x_n} \frac{\delta(x - x_n)}{|df/dx_n|},$$

where x_n are the zeros of the function $f(x)$. For a given $k_\parallel$ there are two values $\pm k_B$ for which $\omega_{\mathbf{k}} = \omega_0$ (see Fig. 3 of Ref. [35]). Then integrating over k_B and the angle ϕ, we get

$$P = 2\pi^3 c^2 \mu^2 \cos^2\psi \int dk_\parallel k_\parallel \left|\frac{dk_B}{d\omega_0}\right| [|A|^2 + |B|^2 + 2\,\mathrm{Re}(A^* B e^{-2iKx_0})]_{\omega_0}. \tag{28}$$

Here ''ω_0'' means that the integrand is evaluated on the equifrequency surface. The derivative preceding the square bracket is found to be

$$\frac{dk_B}{d\omega} = \left.\frac{\partial k_B}{\partial\omega}\right|_K + \left.\frac{\partial k_B}{\partial K}\right|_\omega \left.\frac{\partial K}{\partial\omega}\right|_{k_\parallel} = \frac{\omega}{c^2 K}\frac{F(\omega, K(\omega, k_\parallel))}{\sin k_B d}, \tag{29}$$

$$F(\omega, K(\omega, k_\parallel)) = (1+g)\sin Kd + \alpha(\omega, K)\left(\cos Kd - \frac{\sin Kd}{Kd}\right). \tag{30}$$

Next we evaluate the expression in the square bracket, assuming that K is real. Using Eqs. (23) and (24), after tedious algebra we get

$$[|A|^2 + |B|^2 + 2\,\mathrm{Re}(A^* B e^{-2iKx_0})] = \frac{\omega^2}{8\pi^3 c^2}\frac{\sin Kd - 2\alpha\sin Kx_0 \sin K(d - x_0)}{\left(1 - \dfrac{\alpha}{Kd}\right)\sin Kd + \alpha\cos Kd}. \tag{31}$$

In the regime where K is imaginary, we have to use Eq. (25) instead of Eq. (24). The algebra is different, nevertheless—rather surprisingly—the result is the same as Eq. (31) with the replacement $K \to i|K|$. Hence it is not necessary to separate the integration in Eq. (28) into the regions of $k_\parallel$ smaller and greater than ω/c. Then substituting Eqs. (29) and (31) in Eq. (28), our final result is

$$P = \frac{\mu^2\omega_0^3}{4c^2}\cos^2\psi \int dk_\parallel \frac{k_\parallel |F(\omega_0, K(\omega_0, k_\parallel))|}{|K\sin k_B d|} \times \frac{\sin Kd - 2\alpha\sin Kx_0\sin K(d - x_0)}{\left(1 - \dfrac{\alpha}{Kd}\right)\sin Kd + \alpha\cos Kd}. \tag{32}$$

Here K, α, and F are defined, respectively, by Eqs. (12), (13), and (30) with $\omega = \omega_0$, and $\sin k_B d$ is calculated from Eq. (11). The Bloch wave vector k_B must be real, which is to say that the region of integration must be limited to the values of $k_\parallel$ within the pass bands. Note that the calculation, up to this point, is analytic, and that the desired power is given in terms of a single integration.

Equation (32) gives the power P radiated by a dipole of frequency ω_0, into the TE modes of our model SL. This formula renders P as a function of ω_0, the grating strength g that characterizes the SL, the distance of the dipole x_0 from one of the ''barriers,'' and the angle ψ that the dipole forms with the plane of the barriers. This last dependence is given simply by the factor $\cos^2\psi$ outside the integral. Then, as can be expected, no TE radiation is emitted if the dipole is parallel to the SL axis. It is convenient to work with the normalized dipole position x_0/d, the normalized frequency $\omega_0 d/c$, and the power normalized with the power emitted by a dipole in free space $(3c^3/\mu^2\omega_0^4)P$.

VI. SPECIAL CASES

A. The limit $g \to 0$

This limit corresponds to the empty-lattice model, and the dipole is actually radiating in free space. For $g \to 0$ we have that $\alpha \to 0$ and $\sin k_B d \to \sin Kd$. The equifrequency surface becomes a sphere of radius $|\mathbf{k}| = \omega_0/c$, and the integral of Eq. (32) reduces to

$$\int dk_\parallel \frac{k_\parallel}{K} = \int_0^{\omega_0/c} dk_\parallel \frac{k_\parallel}{\sqrt{\omega_0^2/c^2 - k_\parallel^2}} = \frac{\omega_0}{c}.$$

Then the normalized power becomes

$$\frac{P}{P_0} \to \frac{3c^3}{\mu^2 \omega_0^4} \frac{\mu^2 \omega_0^3}{4c^2} \cos^2 \psi \, \frac{\omega_0}{c} = \frac{3}{4} \cos^2 \psi. \tag{33}$$

In the planned sequel [34] to this paper we will see that, for $\psi = 0$ and $\psi = \pi/2$ this just completes the total—TE plus TM—radiated power to $P/P_0 = 1$, as it should be.

B. The limit $\omega \to 0$

In this low-frequency limit, we can see from the band structure (Fig. 2 of Ref. [35]) that $k_\parallel$ and k_B are also very small. Therefore, $\omega_0 d/c \ll 1$, $k_B d \ll 1$, and $Kd \ll 1$, and $F(\omega_0, K(\omega_0, k_\parallel)) \cong (1+g)Kd$. Further, a series expansion of the dispersion relation (11) reveals that, in this limit,

$$k_B^2 + k_\parallel^2 = (\epsilon_0 + g)\omega^2/c^2. \tag{34}$$

The equifrequency surfaces are again spheres, now of radius $(\epsilon_0 + g)^{1/2}\omega/c$. Then (with $\epsilon_0 = 1$) the integral of Eq. (32) reduces to

$$\begin{aligned}(1+g)\int dk_\parallel \frac{k_\parallel}{k_B} &= (1+g)\int_0^{\sqrt{1+g}(\omega_0/c)} dk_\parallel \\ &\quad \times \frac{k_\parallel}{[(1+g)\omega^2/c^2 - k_\parallel^2]^{1/2}} \\ &= (1+g)^{3/2}\frac{\omega_0}{c}.\end{aligned}$$

Taking into account the prefactor of the integral (32) and the normalizing divisor P_0 [see Eq. (33)] the result is

$$\frac{P}{P_0} \to \frac{3}{4}(1+g)^{3/2}\cos^2 \psi. \tag{35}$$

This, of course, reduces to Eq. (33) for $g \to 0$.

C. Gas of dipoles

Here we assume that a random gas of radiating dipoles fills the spaces between the barriers. In order to obtain the radiated power per dipole, we have to average over all possible directions in space of the dipole moment $\boldsymbol{\mu}$, that is over the angles. This simply replaces the $\cos^2 \psi$ in Eq. (32) by its *volume* average $\frac{1}{3}$.

We also average over the dipole positions x_0. For the position-dependent factor in Eq. (32) we find that

$$\begin{aligned}&\langle \sin Kd - 2\alpha \sin Kx_0 \sin K(d - x_0)\rangle \\ &\quad = \sin Kd + \alpha \cos Kd - \alpha\langle \cos K(d - 2x_0)\rangle \\ &\quad = \sin Kd + \alpha \cos Kd - \alpha \sin Kd/Kd.\end{aligned}$$

This just cancels out a factor in the denominator of the integrand. Then the final result for the radiated power per dipole is

$$\frac{P}{P_0} = \frac{1}{4}\frac{c}{\omega_0}\int dk_\parallel \frac{k_\parallel |F(\omega_0, K(\omega_0, k_\parallel))|}{|K \sin k_B d|}. \tag{36}$$

VII. RESULTS AND DISCUSSION

The integration in Eq. (32) must be carried out carefully, for every value of ω_0, in coordination with the corresponding equifrequency surface. These are given in Ref. [35] (Fig. 3) for $g = 0.1$ and four selected frequency values. Of course, the integration is to be interrupted whenever a gap occurs in $k_\parallel$, and the limiting points must be approached carefully, in small steps. This is because $\sin k_B d$ in the denominator of the integrand vanishes at all the band edges. Nevertheless, this is a weak singularity, and the integral converges. Specifically, for a given ω, one or more bands $\omega_n(k_\parallel)$ are traversed; these are separated by band gaps, namely, regions of $k_\parallel$ for which the characteristic equation has no real solutions for the Bloch vector k_B (see Fig. 2 of Ref. [35]). The integration is then performed separately for every band, as defined by the initial (k_i) and final (k_f) values of $k_\parallel$ for that band n. We have divided the ranges $[k_f^{(n)} - k_i^{(n)}]d$ into 10^5 equal intervals $(\Delta k_\parallel)$; the integration was executed from the value $k_i^{(n)}d + \Delta k_\parallel$ to the value $k_f^{(n)}d - \Delta k_\parallel$ (the points $k_i^{(n)}d$ and $k_f^{(n)}d$ themselves were excluded because of the aforementioned singularity).

In Fig. 2 we plot the normalized (to free space) power radiated by a point dipole whose dipole moment $\boldsymbol{\mu}$ is parallel to the barriers ($\psi = 0$). Three positions of the dipole are considered, namely, when it is at one-half, one-third, and one-quarter of the barrier separation d. For each of these cases the grating strength g assumes two values 0.1 and 0.9, giving rise to relatively weak and to rather strong Bragg diffraction, respectively. First let us note that, in comparison to the case $g = 0.9$, the pattern is rather flat for $g = 0.1$, and oscillates near the value $P/P_0 = 0.75$, independently of ω and x_0. This value, in fact, was derived analytically in the limit $g \to 0$ in the previous section. In the same section we also found the low-frequency limit $P/P_0 = 0.75(1+g)^{3/2}$ for $\psi = 0$ which, for $g = 0.1$ and $g = 0.9$, assumes the values 0.865 and 1.964, respectively. In Fig. 2 we see that these limits are obeyed, indeed, irrespective of the value of x_0.

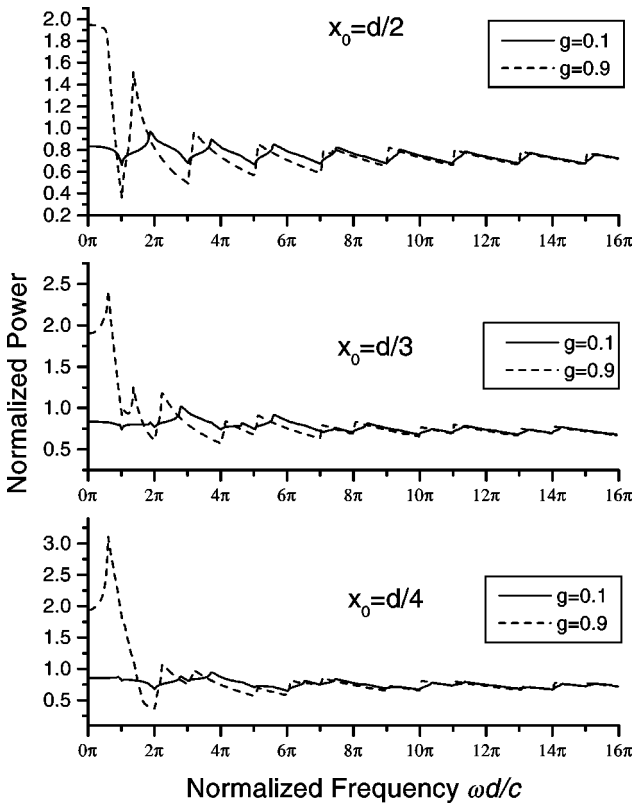

FIG. 2. TE-polarized power radiated by a dipole in the configuration of Fig. 1, as a function of frequency. The frequency is normalized with c/d and the power is normalized with that emitted in free space, $\mu^2\omega^4/3c^3$. The dipole is taken to be parallel to the barriers ($\psi=0$), located midway between two barriers (top), at one-third of the separation (middle), and at one-fourth of the separation (bottom) from either side. Two grating strengths are considered: $g=0.1$ (weak modulation) and $g=0.9$ (strong modulation). Discontinuities in the slope occur at the band edges (for $k_{\|}=0$, namely, axial propagation). Also, notable enhancement ($P\gtrsim 2$) is obtained for low frequencies.

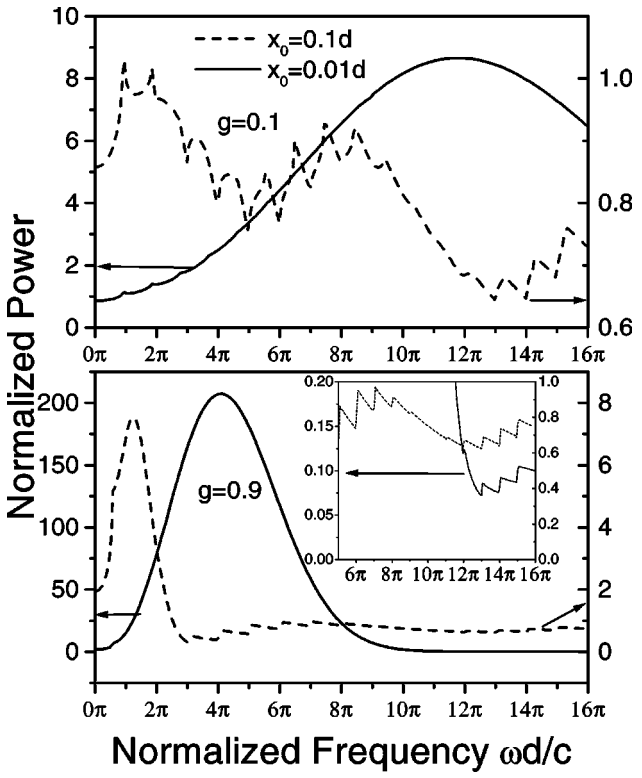

FIG. 3. As Fig. 2, for dipole positions very close to a barrier. The peaks correspond to strong enhancement, which is greater the closer the dipole is to a barrier, and the stronger the modulation (grating strength) is. Note the different scales for $g=0.1$ (right, dashed lines) and $g=0.9$ (left, solid lines). The inset amplifies the high-frequency region for $g=0.9$.

The power spectrum is a succession of more or less sharp minima and maxima. Many of these occur at or near the frequencies $\omega d/c=\pi n$, where n is an integer, independently of g and x_0. We recall that, for the Dirac comb model, the upper band-gap edges (at $k_{\|}=0$) happen to be ''pinned'' at precisely these frequencies. Some of the sharp peaks correspond to lower band-gap edges. Thus, the abrupt changes in the power spectrum seem to be associated with the changes in density of states as the threshold between a pass band and a stop band is traversed. We recall (see Fig. 4 of Ref. [36], which corrects Fig. 5 of Ref. [35]) that the density of states, indeed, exhibits discontinuities of the slope at the band-gap edges. Nevertheless, the power spectrum depends strongly on the position of the dipole while, of course, the density of states is independent of x_0. The differences are seen to be specially notable for lower frequencies.

For $x_0=d/2$ the pattern is repeated with a period 2π, however, no repetitive behavior is apparent for $x_0=d/3$ and $x_0=d/4$. The amplitude of the fluctuation is attenuated as the frequency increases, and seems to approach the high-frequency limit $P/P_0\rightarrow 3/4$. Unfortunately, we were unable to derive this value from Eq. (32). It is notable that it coincides with our result in the limit $g\rightarrow 0$, irrespective of g and x_0. Apparently, for very large frequencies—and very small wavelengths—the wave ''sees'' the barriers as infinitely separated, which amounts to the same as no barriers at all ($g=0$).

In Fig. 3 we show how the radiated power changes as the dipole approaches the barrier: $x_0=0.1d$ and $x_0=0.01d$. For $g=0.1$ a dramatic change occurs as x_0 is reduced from $0.1d$ to $0.01d$, namely, the zigzagging power spectrum gives way to a strong peak at a normalized frequency of about 12π. The peak already appears for a modest distance, $x_0=0.1$; it also shifts to a much lower frequency. Very near to the barrier ($x_0=0.01$) the peak grows by a factor 30 approximately, and the power radiated by the dipole is more than 200 times greater than that in the vacuum. The inset demonstrates that even for large frequencies, the oscillations related to the band edges still continue, although on a minor scale.

Finally, in Fig. 4 we show the power emitted by a gas of dipoles between the barriers. The calculation is based on Eq. (36). The characteristic slope discontinuities are still notable, although not as pronounced as in Fig. 2 for $x_0=0.5$, say. It is interesting that the smoothed-out power increases linearly with frequency, and much more rapidly for $g=0.9$ than for $g=0.1$.

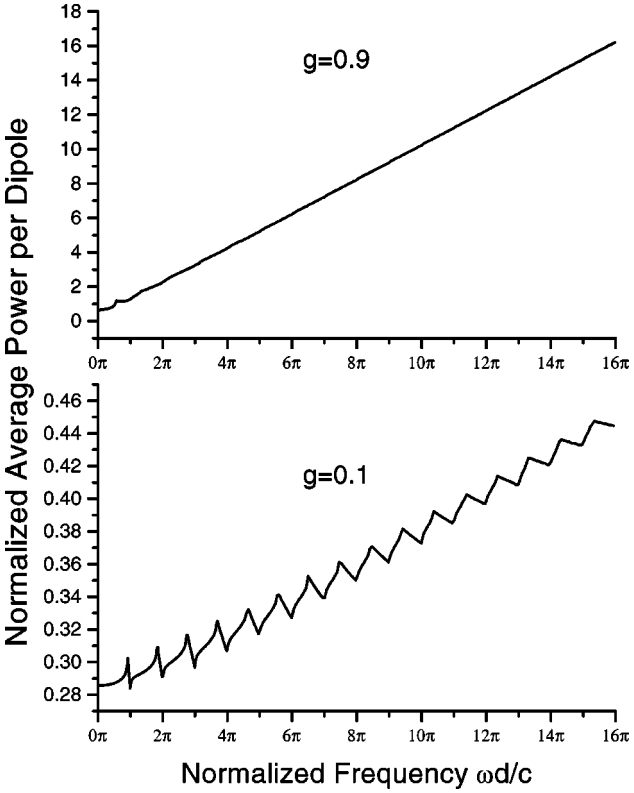

FIG. 4. Power spectrum for a gas of dipoles, for two values of the grating strength.

VIII. CONCLUSION

In this paper we have investigated the power emitted by a point dipole embedded in a model SL. An important feature of our work is the fact that the dipole is permitted to radiate in all spatial directions, although here the polarization was restricted to the TE mode. Because a SL does not have an omnidirectional PBG, the radiation may be *inhibited* in certain frequency regions, but never prohibited. Indeed, we find (see Fig. 2) that the radiated power is finite for all frequencies. What is more, for some frequency ranges, the power is substantially enhanced in comparison to radiation in free space. For dipole positions that are *not* very near to the barriers, the power spectra oscillate around the free-space value (for TE polarization) with an attenuating amplitude as the frequency increases. The most notable property of these spectra are the sharp discontinuities in slope. These occur, predominantly, at frequencies that coincide with the band edges for on-axis propagation; previously we noted the same aspect of the DOS spectra [35]. However, this is as far as the analogy goes. The slope discontinuities in the power spectra do not show up at all the band edges, occasionally they do not coincide with a band edge, and these spectra depend strongly on the dipole position x_0 and on the grating strength g.

The behavior of the power spectrum undergoes a dramatic, qualitative change as the dipole approaches a barrier. Namely, at relatively low frequencies, a large peak appears (see Fig. 3). The smaller x_0 and the greater g, the greater is the enhancement of the emitted power. For example, if $x_0 = 0.01d$ and $g = 0.9$, the enhancement factor is more than 200—a powerful Purcell effect. At this point it should be emphasized that, in our calculation, the dipole is permitted to radiate in all directions in space; the associated DOS (which is also a result of integration over all spatial directions) [35] is *not* large at the band edges, but only exhibits slope discontinuities. This situation contrasts with the DOS for propagation limited to the SL axis [20], which is inversely proportional to the group velocity $d\omega/dk_B$ and, hence, is infinitely large at the band edges. In the present case, the large power enhancement in Fig. 3 does *not* seem to be related to the slope discontinuities of the DOS [35].

We offer a *tentative* interpretation for this unexpectedly large power emission for dipole positions that are close to a barrier. It turns out that a disproportionately large contribution to the power integral Eq. (32) comes from ''terminal'' values of the parallel component of the wave vector. By this we mean, values of $k_\parallel$ very near to the maximum possible for a given frequency; see Fig. 2 of Ref. [35]. Now, in this regime, $k_\parallel$ is actually greater than the vacuum wave vector ω/c, as discussed in Ref. [35]; this is known to occur for a realistic SL as well. As a result, K, as given by Eq. (12), is purely imaginary for a small range of $k_\parallel$ which, however, contributes substantially to the total power. Then, according to Eq. (14), in this range the electric field is evanescent: it decays exponentially away from the barriers. So, the coupling of the dipole to the field is expected to increase rapidly as the dipole approaches a barrier. This argument possibly explains the behavior seen in Fig. 3.

Admittedly, the Dirac comb model that we employed, does not resemble a real SL. Nevertheless, let us recall that this model corresponds to a limiting case of the ordinary SL: very large dielectric constant ϵ (of the higher-index layers) and very small thickness Δ of these layers, the ratio $\epsilon\Delta/d$ being a finite number (g) [35]. If these requirements are satisfied (say, with $\epsilon = d/\Delta = 15$), then we expect our results to have semiquantitative validity. What is more, we believe that our *qualitative* findings are applicable to the power spectra of real SLs. This is because the TE band structure, derived from the Dirac comb model, is qualitatively very similar to that obtained from a realistic modeling of the SL [35]. So, we expect that experimental spectra, for TE polarization, will exhibit slope discontinuities at the band edges for on-axis propagation, and that they will depend substantially on the dipole position—including considerable enhancement of the emitted power. Computer simulation, as well as experimentation, would be desirable.

ACKNOWLEDGMENTS

We wish to thank Jorge R. Zurita for helpful discussions. This work was supported by CONACyT Grant No. 32191-E. also, I.A.R. and A.S.S. were financially supported by CONACyT and Sistema Nacional de Investigadores.

[1] E. M. Purcell, Phys. Rev. **69**, 681 (1946).
[2] D. Meschede, Phys. Rep. **211**, 201 (1992); Y. Yamamoto and R. E. Slusher, Phys. Today **46**, 66 (1993).
[3] Magnus Höijer and Gunnar Björk, Opt. Commun. **150**, 319 (1998); S. Robert, H. Rigneault, and F. Lamarque, J. Opt. Soc. Am. B **15**, 1773 (1998); J. M. Gérard, B. Sermage, B. Gayral, B. Legrand, E. Costard, and V. Thierry-Mieg, Phys. Rev. Lett. **81**, 1110 (1998).
[4] John D. Joannopoulos, Robert D. Meade, and Joshua N. Winn, Photonic Crystals (Princeton University Press, Princeton, 1995).
[5] Eli Yablonovitch, Phys. Rev. Lett. **58**, 2059 (1987).
[6] E. Yablonovitch, T. J. Gmitter, and R. Bhat, Phys. Rev. Lett. **61**, 2546 (1988).
[7] Sajeev John and Jiang Wang, Phys. Rev. Lett. **64**, 2418 (1990); Phys. Rev. B **43**, 12 772 (1991).
[8] A. G. Kofman, G. Kurizki, and B. Sherman, J. Mod. Opt. **41**, 353 (1994).
[9] T. W. Mossberg and M. Lewenstein, J. Opt. Soc. Am. B **10**, 340 (1993); Sajeev John and Tran Quang, Phys. Rev. A **50**, 1764 (1994); B. Sherman, A. G. Kofman, and G. Kurizki, Appl. Phys. B **60**, S99 (1995); S.-Y. Zhu, H. Chen, and H. Huang, Phys. Rev. Lett. **79**, 205 (1997); Tran Quang and Sajeev John, Phys. Rev. A **56**, 4273 (1997); A. Leclair, Ann. Phys. (N.Y.) **271**, 268 (1999); K. Molmer and S. Bay, Phys. Rev. A **59**, 904 (1999).
[10] G. Kurizki, Phys. Rev. A **42**, 2915 (1990).
[11] Jonathan P. Dowling and Charles M. Bowden, J. Opt. Soc. Am. B **10**, 353 (1993).
[12] J. Wang, Phys. Lett. A **204**, 54 (1995).
[13] Sajeev John and Tran Quang, Phys. Rev. Lett. **74**, 3419 (1995).
[14] Tran Quang, Mestin Woldeyohannes, Sajeev John, and Girish S. Agarwal, Phys. Rev. Lett. **79**, 5238 (1997); Mestin Woldeyohannes and Sajeev John, Phys. Rev. A **60**, 5046 (1999).
[15] H. Huang, X. H. Lu, and S. Y. Zhu, Phys. Rev. A **57**, 4945 (1998).
[16] Alan M. Portis, *Electromagnetic Fields* (Wiley, New York, 1978), p. 669.
[17] V. Weisskopf and E. Wigner, Z. Phys. **63**, 54 (1930).
[18] Zhi-Yuan Li, Lan-Lan Lin, and Zhao-Qing Zhang, Phys. Rev. Lett. **84**, 4341 (2000).
[19] Roy J. Glauber and M. Lewenstein, Phys. Rev. A **43**, 467 (1991).
[20] Jonathan P. Dowling and Charles M. Bowden, Phys. Rev. A **46**, 612 (1992).
[21] I. Alvarado-Rodriguez, P. Halevi, and J. J. Sánchez-Mondragón, Rev. Mex. Fis. **44**, 268 (1998).
[22] Michael D. Tocci, Michael Scalora, Mark J. Bloemer, Jonathan P. Dowling, and Charles M. Bowden, Phys. Rev. A **53**, 2799 (1996).
[23] I. S. Fogel, J. M. Bendickson, M. D. Tocci, M. J. Bloemer, M. Scalora, C. M. Bowden, and J. P. Dowling, Pure Appl. Opt. **7**, 393 (1998).
[24] Jonathan P. Dowling, J. Lightwave Technol. **17**, 2142 (1999).
[25] V. P. Bykov, Sov. Phys. JETP **35**, 269 (1972); Sov. J. Quantum Electron. **4**, 861 (1975).
[26] P. St. J. Russell, S. Tredwell, and P. J. Roberts, Opt. Commun. **160**, 66 (1999).
[27] M. Babiker *et al.*, Superlattices Microstruct. **22**, 121 (1997); A. Kamli, M. Babiker, A. Al-Hajry, and N. Enfati, Phys. Rev. A **55**, 1454 (1997).
[28] T. Suzuki, P. K. L. Yu, D. R. Smith, and S. Schultz, J. Appl. Phys. **79**, 582 (1996).
[29] R. K. Lee, O. J. Painter, B. D'Urso, A. Scherer, and A. Yariv, Appl. Phys. Lett. **74**, 1522 (1999).
[30] M. Boroditsky, T. F. Krauss, R. Coccioli, R. Vrijen, R. Bhat, and E. Yablonovitch, Appl. Phys. Lett. **75**, 1036 (1999).
[31] T. Baba, K. Inoshita, H. Tanaka, J. Yonekura, M. Ariga, A. Matsutani, T. Miyamoto, F. Koyama, and K. Iga, J. Lightwave Technol. **17**, 2113 (1999).
[32] Toshio Suzuki and Paul K. L. Yu, J. Opt. Soc. Am. B **12**, 570 (1995).
[33] Jordi Martorell and N. M. Lawandy, Phys. Rev. Lett. **65**, 1877 (1990); Takashi Yamasaki and Tetsuo Tsutsui, Appl. Phys. Lett. **72**, 1957 (1998); E. P. Petrov, V. N. Bogomolov, I. I. Kalosha, and S. V. Gaponenko, Phys. Rev. Lett. **81**, 77 (1998); A. Blanco, C. López, R. Mayoral, H. Míguez, F. Meseguer, A. Mifsud, and J. Herrero, Appl. Phys. Lett. **73**, 1781 (1998); Yu. A. Vlasov, K. Luterova, I. Pelant, B. Hönerlage, and V. N. Astratov, Thin Solid Films **318**, 93 (1998); K. Yoshino *et al.*, Jpn. J. Appl. Phys. **237**, L1187 (1998); K. Yoshino, S. B. Lee, S. Tatsuhara, Y. Kawagishi, M. Ozaki, and A. A. Zakhidov, Appl. Phys. Lett. **73**, 3506 (1998); K. Yoshino, S. Tatsuhara, Y. Kawagishi, M. Ozaki, A. A. Zakhidov, and Z. V. Vardeny, *ibid.* **74**, 2590 (1999); M. Megens, J. E. G. J. Wijnhoven, A. Legendijk, and W. L. Vos, Phys. Rev. A **59**, 4727 (1999); S. V. Gaponenko, V. N. Bogomolov, E. P. Petrov, A. M. Kapitonov, D. A. Yarotsky, I. I. Kalosha, A. A. Eychmueller, A. L. Rogach, J. McGilp, U. Woggon, and F. Gindele, J. Lightwave Technol. **17**, 2128 (1999); S. G. Romanov, T. Maka, C. M. S. Torres, M. Muller, and R. Zentel, *ibid.* **17**, 2121 (1999).
[34] Jorge R. Zurita and P. Halevi (unpublished).
[35] I. Alvarado-Rodriguez, P. Halevi, and J. J. Sánchez-Mondragón, Phys. Rev. E **59**, 3624 (1999).
[36] Jorge R. Zurita and P. Halevi, Phys. Rev. E **61**, 5802 (2000).